HiSST: International Conference on
High-Speed Vehicle Science Technology
26–29 November 2018, Moscow, Russia

Novel Transient Calorimetric Heat Flux Sensor in Hypersonic Ground Experiment

Shizhong Zhang [1], Jinping Li [2], Hong Chen [3], Xiaoyuan Zhang [4] , Hongru Yu [5]

Abstract

The accurate prediction of aerodynamic heating environment can effectively reduce the margin of thermal design and increase the payload, while the ground wind tunnel experiment is an important means to predict the aerodynamic heating environment. The existing transient heat flux sensors in hypersonic ground wind tunnel experiment include thin film thermometer and coaxial thermocouple. The former has high sensitivity, but it is not suitable for occasions where airflow is severely damaged; the latter is resistant to erosion, but the sensitivity is low, and the response characteristic is susceptible to the fine structure of the nodes, therefore it is only suitable for high heat flux measurement. In order to improve the accuracy of aerodynamic heating measurement, new heat flux measurement methods should be continuously developed. This paper presents a novel transient calorimetric heat flux sensor using diamond chips to replace the commonly used copper pieces as the calorimetric sheet. The temperature on back side of the calorimeter is measured by a thin film thermometer, which can greatly improves the output sensitivity of the calorimeter. The sensor design and selection of characteristic parameters is with the help of theoretical analysis and numerical calculation. The fabricated sensors have high linearity with temperature. The experimental results show that the repeatability error of the transient calorimetric heat flux sensor is within 4% and the error of measurement accuracy is within 6%. The sensor resistance keeps unchanged in the multi-tested and the measurement result is accurate and reliable.

Keywords: aerodynamic heat transfer， transient measurement, calorimetric heat flux sensor, diamond, shock wave wind tunnel

Nomenclature

T_0 – Initial temperature
T_b– Back surface temperature
F_o– Fourier number
c – Specific heat capacity
k – Thermal conductivity
l – Thickness
q_0– Constant surface heat flux
q_b– Back surface heat flux
t_R – Response time
α – Thermal diffusivity
ρ – Density

[1] *Institute of Mechanics, Chinese Academy of Sciences, No.15 Beisihuanxi Road, Beijing, China, zhangshizhong@imech.ac.cn*
[2] *Institute of Mechanics, Chinese Academy of Sciences, No.15 Beisihuanxi Road, Beijing, China, lijinping@imech.ac.cn*
[3] *Institute of Mechanics, Chinese Academy of Sciences, No.15 Beisihuanxi Road, Beijing, China, hongchen@imech.ac.cn*
[4] *Institute of Mechanics, Chinese Academy of Sciences, No.15 Beisihuanxi Road, Beijing, China, zhangxiaoyuan@imech.ac.cn*
[5] *Institute of Mechanics, Chinese Academy of Sciences, No.15 Beisihuanxi Road, Beijing, China, hryu@imech.ac.cn*

Copyright © 2018 by the author(s)

1. Introduction

With the development of adjacent spacecraft, the flight time of the aircraft in the atmosphere is lengthened, and the problem of aerodynamic heating load becomes more prominent. Micro-ablative or non-ablative materials are required to ensure that the shape of the aircraft is basically unchanged, so high requirements are placed on the thermal protection design, which is required to meet the thermal protection problem of the aircraft during long flight. The aerodynamic thermal environment is the premise for the selection of heat-resistant materials and the design of heat-proof structures. Therefore, high requirements are also placed on the prediction of the thermal environment of aircraft. Accurate prediction of aerodynamic thermal environment is an important basis for thermal protection structure design and material selection, which can effectively reduce the margin of heat protection design, reduce the quality of heat protection structure, and increase the payload [1].

There are three main methods for aerodynamic heating research: numerical calculation, flight test and ground wind tunnel test. Since there is no good solution to the accuracy of the numerical calculation of aerodynamic heating and the problem of grid dependence, it is still necessary to test the correctness of the numerical calculation results through experiments [2]. The temperature rise of the structural components of the aircraft during the flight test is high, the influence of thermal radiation on the measurement results of the heat flux is the biggest source of measurement error. The three-dimensional characteristics of the flight test flow field and the structure are also not conducive to the accurate prediction of aerodynamic heat flux [3]. The cost of flight test is very high, so the ground wind tunnel test is still the main means to carry out aerodynamic thermal environment research [4][5] .

The heat flux measurement in ground wind tunnel test is divided into transient heat flux measurement and conventional heat flux measurement. The transient heat flux measurement time is very short, the wall temperature rise is small, and the wall temperature can be approximated, so the transient heat flux measurement provides the cold wall heat flux. The cold wall represents the most severe load determined by the flow field and the shape of the aircraft under the material-free heat protection mechanism [6], which is an important basis for the design of the aircraft. Conventional measurement time is long, the surface temperature of the model increases, and the changing wall temperature brings difficulties to the experimental measurement of heat flux [7]. At the same time, the temperature rise will cause the thermal property parameters of the material to change [8], thus affecting the accuracy of heat flux measurement. Therefore, the aerodynamic heating test is not as effective as the longer the test time, and the transient heat flux measurement is more advantageous.

Transient heat flux measurement also has advantages in the aerodynamic thermal environment test. Transient heat flux measurement requires no special cooling system due to its short flow time. The design and manufacture of the model is relatively simple. The temperature rise of the model during the test is small. It is believed that the wall temperature of the model remains basically unchanged during the test, which greatly simplifies the data processing [9].

There are three main types of transient heat flux sensors: thin film resistance thermometers, coaxial thermocouples and copper calorimeters [10]. The film resistance thermometer was firstly applied, its sensitivity is high, but the film thickness is very thin, the structural and physical parameters are unstable. The reliability of measurement is difficult to improve, and it is not suitable for the measurement of airflow scouring and airflow conduction. Coaxial thermocouples have made remarkable progress in recent years [11], and the performance meets the requirements for use, but the sensitivity is low. The existing copper foil calorimeter uses a thermal couple to measure the back surface temperature. Although it is resistant to scouring, the sensitivity is not high, and the thermocouple contact technique is difficult, which hinders the accuracy of the measurement data from further increasing.

The purpose of this study was to create a transient calorimetric heat flux sensor with a greatly improved sensitivity. If the calorimeter back temperature measuring element is changed from thermocouple to thin film resistance thermometer, the sensitivity of the sensor can be greatly improved. However, the existing calorimeter uses copper foil as a calorimetric sheet. The copper has

Copyright © 2018 by the author(s)

high thermal conductivity, which satisfies transient calorimeter requirements, but it also has high electrical conductivity, which hinders the use of thin-film resistance thermometer as the back-side temperature measuring elements. The key to this study is to find a material with good thermal conductivity and good electrical insulation. After exploration, it was proposed to use diamond chips to replace the commonly used copper pieces as the calorimetric sheet, which greatly improved the output sensitivity of the transient calorimeter.

The new transient heat flux sensor can not only solve the problem in the case of low heat flux and strong scouring that no sensor is available, but also cover a wider range of heat flux measurement. Meanwhile, the sensor is in contact with the air flow with non-metallic materials, which can facilitate the study of aerodynamic heating under dissociation conditions. The new sensor has a wide range of applications.

2. Design principle of transient calorimetric heat flux sensor

2.1. Sensor structure design

Schematic diagram of the transient calorimetric heat flux sensor is shown in Fig.1. First, a platinum film is sputtered on the back of the calorimeter as a temperature sensing component, and then the calorimeter is mounted on the sensor base. Platinum film wires are taken out from the back of the calorimeter, and the backing is filled with air or epoxy. The measuring principle of the calorimeter is to assume that there is no heat loss on the back side and the side surface of the calorimeter. The heat transferred into the calorimeter per unit area at a certain time interval should be equal to the heat accumulated in the calorimeter. The rate of temperature change can be used to determine the heat flux. In actual measurement, the average temperature is difficult to measure, generally the back surface temperature is measured instead of the average temperature [12]. In this design, the platinum film resistance is used to measure the temperature of the back surface of the measuring calorimeter, which output sensitivity is high.

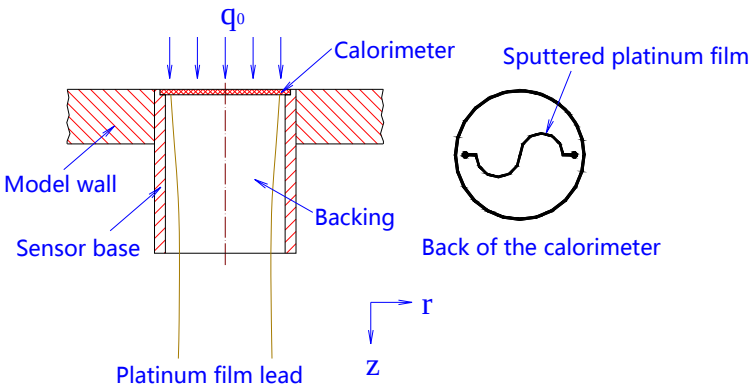

Fig 1. Structural diagram of the transient calorimetric heat flux sensor

The selection of calorimetric sheet materials is the key to the development of new sensors. For transient heat flux measurement, the thermal response time of the calorimeter is required to be fast; the electrical insulation of the back surface is required to be good for sputtering platinum film. In this design, the diamond piece is used as the calorimeter. The thermal conductivity of diamond can reach $1800W/(m \cdot K)$, which is about 5 times of the thermal conductivity of copper, and its resistivity is greater than $10^{14}\Omega \cdot cm$. It can meet the requirements of high thermal conductivity and high resistivity of the calorimeter in design at the same time, so is an ideal calorimetric sheet material. Natural diamonds are expensive, but in recent years, the research on synthetic diamond membranes has been very extensive. The diamond membranes are usually synthesized by low pressure or atmospheric pressure chemical vapor deposition (CVD) [13], which can greatly reduce the cost.

2.2. Thermal response characteristics of the sensor

The response time of the sensor is only related to the thermal response characteristics of the calorimeter material. It can be simplified to the one-dimensional infinite heat conduction problem according to the working principle of the calorimeter under ideal conditions.

Copyright © 2018 by the author(s)

Assuming an infinite plate with a thickness of *l*, the initial temperature is $T_0$and the surface is heated by a constant heat flux q_0. The back is insulated. The temperature distribution field [14] at any time and at any position is:

$$T(x,t) = T_0 + \frac{q_0 l}{k}\left(\frac{\alpha t}{l^2} + \frac{1}{3} + \frac{x^2}{2l^2} - \frac{x}{l} - \frac{2}{\pi^2}\sum_{n=1}^{\infty}\frac{1}{n^2}cos(\frac{n\pi x}{l})e^{-\alpha\left(\frac{n\pi}{l}\right)^2 t}\right) \quad (1)$$

Where $\alpha = \frac{k}{\rho c}$c is the thermal diffusivity of the material, *k* is the thermal conductivity, ρ is the density, and c is the specific heat capacity.

When t reaches a certain level, the internal heat flux of the plate is equal everywhere:

$$\frac{\partial T(x,\infty)}{\partial t} = \frac{q_0}{\rho c l} = constant \quad (2)$$

Eq.2 is the basic principle of calorimeter measurement.

The back temperature $\mathrm{T_b}$ is calculated as:

$$\mathrm{T_b = T(l,t) = T_0 + \frac{q_0 t}{\rho c l} - \frac{1}{6}\frac{q_0 l}{k} + \frac{2q_0 l}{k\pi^2}\sum_{n=1}^{\infty}\frac{(-1)^n}{n^2}e^{-\alpha\left(\frac{n\pi}{l}\right)^2 t}} \quad (3)$$

Back temperature change rate:

$$\frac{dT_b}{dt} = \frac{q_0}{\rho c l}\left(1 + 2\sum_{n=1}^{\infty}(-1)^n e^{-\alpha\left(\frac{n\pi}{l}\right)^2 t}\right) \quad (4)$$

The first term and the second term of Eq.3 are the average temperature T_{ave} of the calorimeter. The first term of Eq.4 is the average temperature change rate of the calorimeter $\frac{dT_{ave}}{dt}$. The series terms of the Eq.3 and Eq.4 converge quickly. The temperature rise on the back of the calorimeter $\Delta T_b = T_b - T_0$, the average temperature rise $\Delta T_{ave} = T_{ave} - T_0$. The ratio of the back temperature rise rate to the average temperature rise rate shown in Table 1:

Table 1. The ratio of the back temperature rise rate to the average temperature rise rate

$F_0 = \alpha t/l^2$	$\Delta T_b/\Delta T_{ave}$	$\frac{dT_b}{dt}\Big/\frac{dT_{ave}}{dt}$
0.1	8%	25%
0.3	47.7%	90%
0.5	67%	98.60%
1	83%	99.99%

It can be seen from the Table 1 that when the Fourier number F_0 is the same, the ratio of the back surface temperature change rate to the average temperature change rate is better than the ratio of the back surface temperature to the average temperature, that is, the back surface temperature change rate versus the average temperature change rate is more casual than the temperature change itself. When$F_0 = \alpha t/l^2 > 0.5$, the difference of the back temperature changes is less than 1.4%. Fortunately, the calorimeter calculation just requires the back temperature change rate. Therefore, when determining the steady heat flow, the error caused by the back temperature measurement instead of the average temperature can be ignored as long as $t > 0.5l^2/\alpha$.

The back heat flux q_b is calculated as:

$$q_b = \rho c l\frac{dT_b}{dt} \quad (5)$$

It indicates that once the heat is infiltrated from the surface of the calorimeter to the back side, the sum of the series of terms in Eq.4 can be replaced by the first item of expansion [15]:

$$\frac{dT_b}{dt} = \frac{q_0}{\rho c l} - \frac{2q_0}{\rho c l}e^{-\alpha(\frac{\pi}{l})^2 t} \quad (6)$$

The back heat flux is compared to the theoretical heat flux value as:

Copyright © 2018 by the author(s)

$$\frac{q_b}{q_0} = \frac{(\rho c l \frac{dT_b}{dt})}{q_0} = 1 - 2e^{-\alpha(\frac{\pi}{l})^2 t} = 1 - 2e^{-\alpha(\frac{\pi}{l})^2 t_R} \tag{7}$$

The response time t_R of the sensor is:

$$t_R = \frac{l^2}{\alpha \pi^2} ln(\frac{2}{1-\frac{q_b}{q_0}}) \tag{8}$$

It can be seen from Eq.8 that the response time of the sensor is only related to the thickness of the calorimeter and the thermal diffusivity α of the material.

Fig.2 shows the relationship between response time and thickness of several typical materials with high thermal conductivity. It can be seen that the thinner the calorimeter, the faster the response time, and the diamond has the fastest response time when the thickness is the same. When 0.2mm CVD diamond is used as the calorimeter, the response time of the calorimeter is only 59 microseconds. The thermal frequency of the diamond material is higher than other metal materials. Therefore, the use of diamond as a calorimeter can improve the response speed of the transient calorimeter.

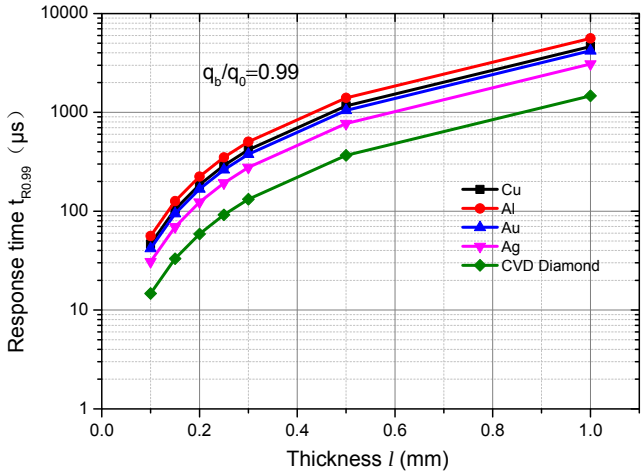

Fig 2. Thermal response characteristics of calorimeter materials

3. The characteristic parameters optimization of the sensor

The characteristic parameters of the sensor mainly include the substrate material, the size of the calorimeter and the size of the base. The characteristic parameters affect the back surface temperature distribution. Therefore, it is necessary to determine the uniform temperature distribution on the back surface of the calorimeter, then sputter the platinum film resistance in the uniform region to ensure the accuracy of the measurement results.

The thermal diffusion caused by different diameters, pedestals and backing materials has different effects on the measurement results. These factors are coupled with each other, making theoretical analysis is difficult. In order to analyze and optimize the design, the numerical simulation method is used to analyze the heat conduction process of the sensor. The control equation uses the following two-dimensional unsteady heat conduction differential equation:

$$\frac{\partial T(r,z,t)}{\partial t} = \frac{k_i}{\rho_i c_i}\left(\frac{\partial^2 T}{\partial r^2} + \frac{1}{r}\frac{\partial T}{\partial r} + \frac{\partial^2 T}{\partial z^2}\right)(i = 1,2,3) \tag{9}$$

Where r and z are the radial and axial directions of the sensor center respectively, other parameters are the same as Eq.1, subscripts 1, 2, and 3 respectively represent the calorimeter, base and backing material, as shown in Fig.1.

The temperature and the heat flux continuity condition are met inside the sensor. The boundary conditions at the surface are:

Copyright © 2018 by the author(s)

$$\left(\frac{\partial T}{\partial z}\right)_{z=0} = \frac{q_0}{k_i}(i = 1,2); t > 0 \quad (10)$$

Other surfaces are treated as adiabatic conditions. The solution of Eq.9 uses a second-order precision finite difference in the spatial direction and a fourth-order Runge-Kutta algorithm in the time direction.

Taking into account the size requirements of the sensor in the actual application, the calculated diameter D of the sensor in this example is 20mm, 10mm and 5mm respectively, the insulating material is selected as the insulating air and epoxy resin, and the base material is made of easy-to-process and heat-insulating FRP material. The surface is loaded with a constant heat flux $q_0 = 1MW/m^2$.

The results of the numerical calculations are shown in Fig.3, which is a graph showing the relationship between the backside heat flux value and the theoretically loaded heat flux caused by different gauge diameters and different substrate materials over time. When the backing is air, the heat flux error between the back surface and the theoretical is increased as the diameter of the sensor decreases at the center position. The reason is that when the load heat flux is constant, the heat loss caused by heat dissipation to the base is certain, but the total heat absorbed by different diameters of the heat meter are different. As the diameter of the sensor decreases, the heat loss of this part accounts for a relatively larger proportion of the total heat absorbed by the heat meter, as a result, the heat flux error increases as the diameter decreases. At the same time, it can be seen that the error values of different diameter sensors increase with time. At the time of 12ms calculation, the error value is 0.2%, 2.5%, and 5.2%respectively at D=20mm, D=10mm and D=5mm.

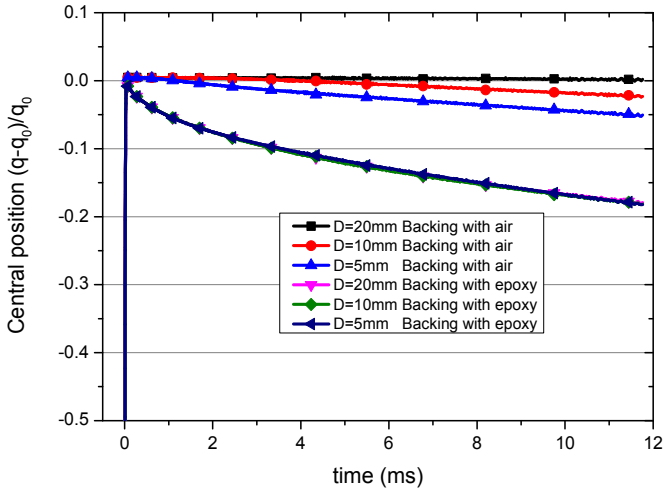

Fig 3. The deviation of the back heat flux to the theoretical heat flux with different diameters at center position

When the backing material is epoxy resin, the heat flux of the three diameter sensors is much lower than the theoretical heat flux, and the maximum error reaches 18% at 12ms, indicating that the measurement error due to the heat dissipation of the epoxy resin is large. The relative error values between the three diameter sensors are not much different, mainly due to the consistent heat loss caused by the back epoxy.

The above calculation results show that when the diameter D=20mm and the backing is air, the difference between the back surface heat flux and the theoretical heat flux is the smallest at the center point position. Select this parameter as the characteristic parameter of the design, and the principle sensor produced is shown in Fig.4.

Copyright © 2018 by the author(s)

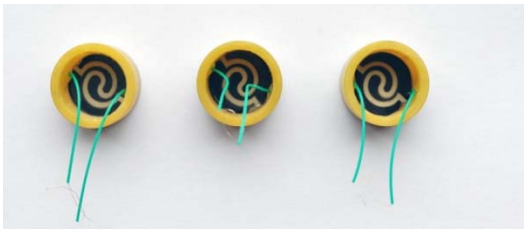

Fig 4. Photos of the transient calorimetric heat flux sensor

The measurement results of the temperature coefficient of resistance show that the linearity coefficient of the platinum film resistance and the temperature is very good for the transient calorimetric heat flux sensor, and the static performance of the sensor is stable.

4. Hypersonic aerodynamic heating measurement verification test

4.1. Test platform and model

The hypersonic aerodynamic heating measurement verification test is carried out on the detonation driven shock wave tunnel. The wind tunnel structure diagram and wave diagram are shown in Fig.5. The drive section length of the shock wave wind tunnel is 15 meters, the initial ratio H2:O2:N2=2:1:2, the absolute pressure is 2.7bar.The driven section length is 11 meters, the gas is air, and the initial pressure is 3800Pa. The Mach number of the nozzle name is 5.5, and the sewing operation state is adopted. The total inlet temperature of the nozzle is 3500K, the total pressure is 12 bar, and the effective pressure platform time is 16ms.

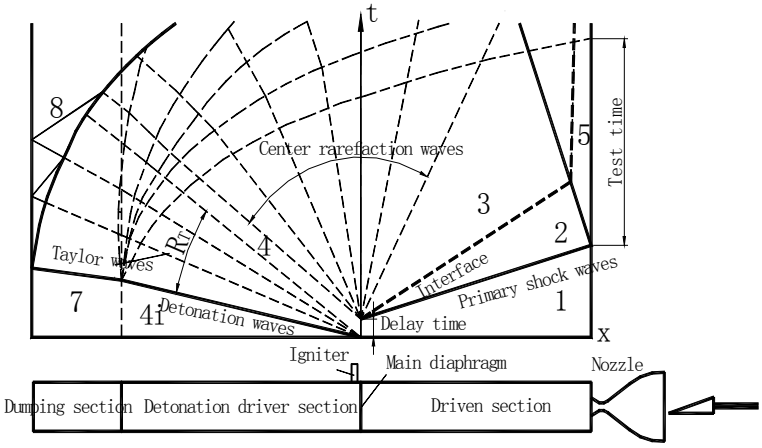

Fig 5. Principle of shock tunnel driven by detonation

Since the plate flow is relatively simple, the theoretical heat flux can be accurately calculated. Therefore, the experimental model uses a 17° wedge, as shown in Fig.6. Three new sensors were evenly mounted on the wedge surface at an angle of 150 mm, 200 mm and 250 mm from the apex, and thin film resistance thermometer and coaxial thermocouple were respectively installed at each corresponding position for comparison.

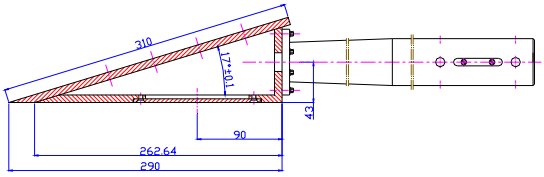

Fig 6. The wedge model for hypersonic aerodynamic heating test

Copyright © 2018 by the author(s)

4.2. Test results and discussion

A total of three repetitive tests were carried out in this test, and the consistency of the three test flow fields was very good. Fig.7 shows the heat flux results measured for three transient heat flux sensors at three different locations in a single test.

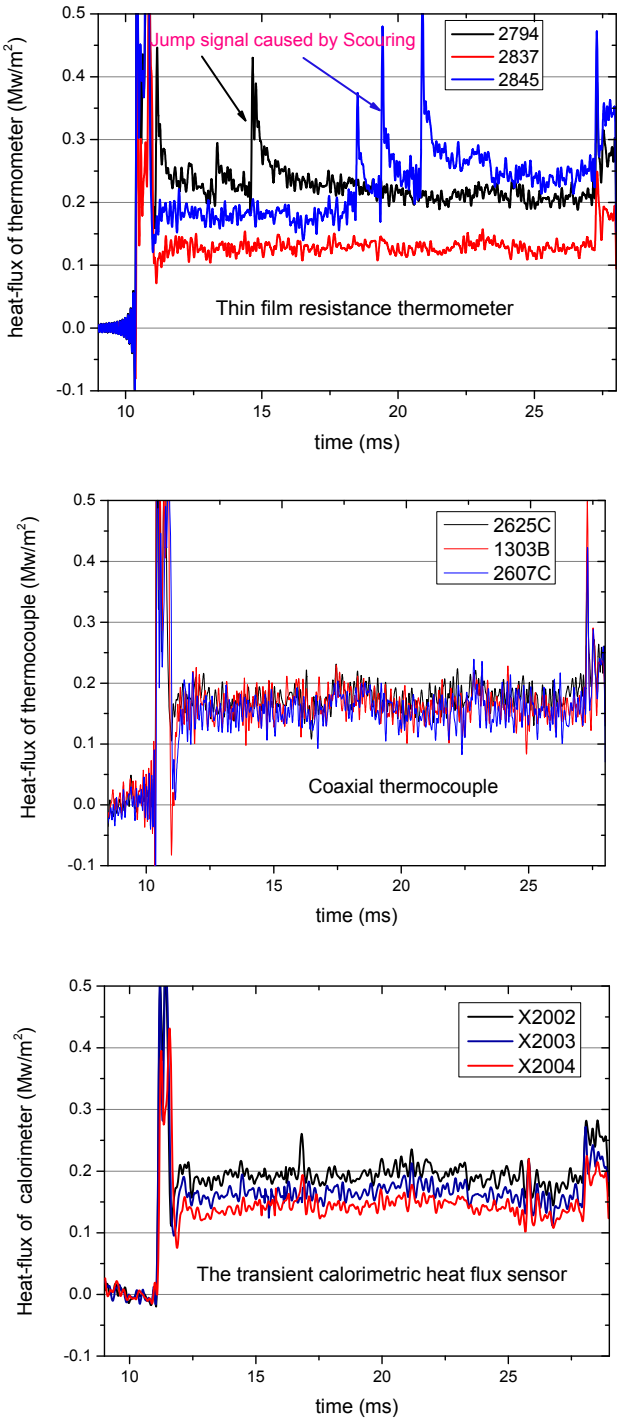

Fig 7. Three transient heat flux sensor measurements during one test

It can be seen from Fig. 7 that the resistance and physical properties of the thin film resistance thermometer change during the airflow scouring process, resulting in a large step signal in the heat flux signal. The jump position is random, and some heat flux value directly deviates from the true

Copyright © 2018 by the author(s)

value after the jump, indicating that the measurement result of the thin film resistance thermometer is not credible.

In this case, the heat flux value of the flat plate is low, the signal-to-noise ratio of the measured signal by the coaxial thermocouple is poor due to the sensitivity of the original output signal. The heat flux signals at three different measuring points overlap together due to the large signal noise, which shows that the coaxial thermocouple has poor measurement accuracy in low heat flux measurement.

The heat flux measured by the transient calorimetric heat flux sensor is relatively stable, and the given heat flux curve versus time can obviously reflect the three stages of flow field initiation, stabilization and end. The heat flux is relatively flat during the effective test time. The heat flux distribution of the three different measuring points is obvious, indicating that the new sensor has a high heat flux identification rate in the case of low heat flux measurement.

Table 2 shows the measured heat flux values of the transient calorimetric heat flux sensor in three tests. The theoretical value is calculated by the reference enthalpy method [16]. It can be seen that the repeatability of the new sensor measurement results is very good, and the measurement accuracy error is within 6%.

Table 2. Experimental results of the transient calorimetric heat flux sensors (MW/m^2)

Point	1	2	3
Run 1	0.19	0.163	0.141
Run2	0.19	0.162	0.140
Run3	0.197	0.17	0.148
Average	0.192	0.165	0.143
Theoretical	0.196	0.170	0.152
Error	2.02%	2.79%	5.81%

In order to investigate the reliability and stability of the sensor, the resistance values of the new sensor and the film resistance thermometer were accurately measured before and after each test. Fig.8 shows the change of the resistance of the sensor during the three tests. It can be seen that the resistance of the thin film resistance thermometer changes after each test, and the sensitivity coefficient of the film changes, which makes the measurement result inaccurate. The resistance of the new transient calorimeter remains stable in all three tests, thus ensuring the reliability of the heat flow measurement results.

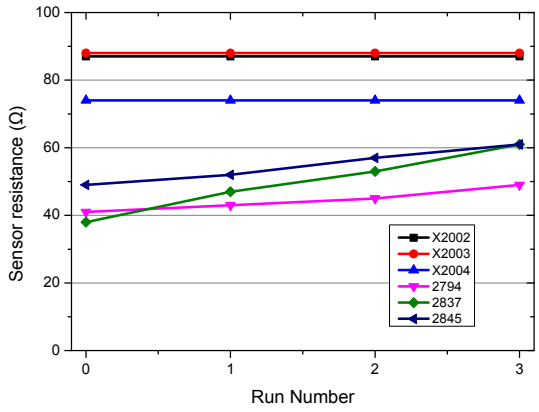

Fig 8. Sensor's resistance change during the experiment

5. Conclusion

This paper creates a novel transient calorimetric heat flux sensor that is both washable and sensitive. The analysis of the thermal response characteristics of the sensor shows that the response time of

Copyright © 2018 by the author(s)

the calorimeter is only related to the thermal diffusivity and thickness of the calorimetric material. Diamond can improve the frequency response of the sensor. The characteristic design parameters of the sensor are determined by numerical calculation of the two-dimensional heat conduction model. The results of the prototype verification sensor in the aerodynamic heating measurement test of the hypersonic shock wave wind tunnel show that the principle of the transient calorimetric heat flux sensor is feasible. The heat flux measurement result is reproducible and reliable, the accuracy error is within 6%.

References

1. Wang Q, Li J P, Zhao W, et al. Comparative study on aerodynamic heating under perfect and nonequilibrium hypersonic flows. Sci China Physics, Mechanics and Astronomy, 59(2): 624701(2016).
2. Peng Zhiyu, Shi Yilei, Gong Hongming et al. Hypersonic aerodynamic thermal prediction technology and its development tren. Acta Aeronautica Sinica, 36(1): 325-345(2015).
3. Neumann R D. Thermal Instrumentation: A State-of-the-Art Review. Thermal Instrumentation: A State-of-the-Art Review (1993).
4. Holden M S, Parker R A. LENS hypervelocity tunnels and application to vehicle testing at duplicated flight conditions, advanced hypersonic test facilities. AIAA Journal, 198: 73-110 (2002).
5. Wu S, Shu Y H, Li J P, et al. An Integral Heat Flux Sensor with High Spatial and Temporal Resolutions[J]. Chin Sci Bull, 59(27): 3484-3489 (2014).
6. Ding Xiaoheng. Research on method and device for measuring heat flux density in hypersonic flight test. Harbin Institute of Technology (2015).
7. Chen Lianzhong. Study on the Correction Method of Measurement Results of Plug-type Transient Calorimeter[J].Acta Metrologica Sinica, 29(4): 317-319 (2008).
8. Hu Wei, Chen Zeyi. Calorimetric Technology and Physical Property Measurement. Hefei: University of Science and Technology of China Press (2009).
9. Hamburger, C.: Quasimonotonicity, regularity and duality for nonlinear systems of partial differential equations. Ann. Mat. Pura Appl. 169, 321–354 (1995).
10. Schultz D L, Jones T V. Heat Transfer Measurements in Short Duration Facilities. AGARD-AG-165, University of Oxford (1973).
11. Li J P, Chen H, Zhang S Z, et al. On the response of coaxial surface thermocouples for transient aerodynamic heating measurements. Experimental Thermal and Fluid Science, , 86: 141-148(2017).
12. Yu Hongru, Li Zhongfa et al. Plug-type copper foil calorimeter for heat transfer measurement of shock wave tunnel. Advances in Mechanics (1976).
13. Yan X B, Wei J J, Guo J C, et al. Mechanism of graphitization and optical degradation of CVD diamond films by rapid heating treatment. Diamond & Related Materials(2016).
14. Corslaw H S, Jaeqer J C. Conduction of heat in solids. Oxford University Press(1959).
15. Hightower T M, Olivares R A, Philippidis D. Thermal Capacitance (Slug) Calorimeter Theory Including Heat Losses and Other Decaying Processes. NASA TM, , 215364(2008).
16. Eckert E R G. Engineering relations for heat transfer and friction in high-velocity laminar and turbulent boundary-layer flow over surfaces with constant pressure and temperature. Transactions of the ASME, 78(6): 1273-1283(1956).

Copyright © 2018 by the author(s)